JOURNAL OF SOLID STATE CHEMISTRY 52, 254–273 (1984)

Unusual Effects of Anisotropic Bonding in Cu(II) and Ni(II) Oxides with K_2NiF_4 Structure[1]

K. K. SINGH, P. GANGULY, AND J. B. GOODENOUGH[2]

Solid State and Structural Chemistry Unit, Indian Institute of Science, Bangalore 560 012, India

Received July 15, 1983

Geometric constraints present in A_2BO_4 compounds with the tetragonal-T structure of K_2NiF_4 impose a strong pressure on the B—O_{II}—B bonds and a stretching of the A—O_I—A bonds in the basal planes if the tolerance factor is $t \equiv R_{AO}/\sqrt{2}\,R_{BO} < 1$, where R_{AO} and R_{BO} are the sums of the A—O and B—O ionic radii. The tetragonal-T phase of La_2NiO_4 becomes monoclinic for Pr_2NiO_4, orthorhombic for La_2CuO_4, and tetragonal-T′ for Pr_2CuO_4. The atomic displacements in these distorted phases are discussed and rationalized in terms of the chemistry of the various compounds. The strong pressure on the B—O_{II}—B bonds produces itinerant $\sigma^*_{x^2-y^2}$ bands and a relative stabilization of localized d_{z^2} orbitals. Magnetic susceptibility and transport data reveal an intersection of the Fermi energy with the $d^2_{z^2}$ levels for half the copper ions in La_2CuO_4; this intersection is responsible for an intrinsic localized moment associated with a configuration fluctuation; below 200 K the localized moment smoothly vanishes with decreasing temperature as the $d^2_{z^2}$ level becomes filled. In La_2NiO_4, the localized moments for half-filled d_{z^2} orbitals induce strong correlations among the $\sigma^*_{x^2-y^2}$ electrons above $T_d \simeq 200$ K; at lower temperatures the $\sigma^*_{x^2-y^2}$ electrons appear to contribute nothing to the magnetic susceptibility, which obeys a Curie–Weiss law giving a μ_{eff} corresponding to $S = 1/2$, but shows no magnetic order to lowest temperatures. These surprising results are verified by comparison with the mixed systems $La_2Ni_{1-x}Cu_xO_4$ and $La_{2-2x}Sr_{2x}Ni_{1-x}Ti_xO_4$. The onset of a charge-density wave below 200 K is proposed for both La_2CuO_4 and La_2NiO_4, but the atomic displacements would be short-range cooperative in mixed systems. The semiconductor–metallic transitions observed in several systems are found in many cases to obey the relation $E_a \simeq kT_{min}$, where $\rho = \rho_0 \exp(-E_a/kT)$ and T_{min} is the temperature of minimum resistivity ρ. This relation is interpreted in terms of a diffusive charge-carrier mobility with $E_a \simeq \Delta H_m \simeq kT$ at $T = T_{min}$.

Introduction

Although oxides with the tetragonal K_2NiF_4 structure were known in the 1950s (*1, 2*), it was not until 1970 that their significance for the study of two-dimensional magnetic properties was fully appreciated (*3*).

Longo and Raccah (*4*) were the first to signal an abrupt change in the c/a ratio on going from orthorhombic La_2CuO_4 to tetragonal Pr_2CuO_4. Ganguly and Rao (*5*) reported that La_2CuO_4 is essentially metallic whereas Sm_2CuO_4 and Nd_2CuO_4, which have the Pr_2CuO_4 structure, are semiconductors. Kenjo and Yajima (*6*) independently reported a similar result and, to explain their data, proposed a configuration change $3d^1_{z^2}4p^0_z \rightarrow 4p^1_z 3d^0_{z^2}$, which presumably implies the crossing of a half-filled, lo-

[1] Communication No. 206 from Solid State and Structural Chemistry Unit.

[2] Permanent address: Inorganic Chemistry Laboratory, South Parks Road, Oxford OX1 3QR, UK.

0022-4596/84 $3.00

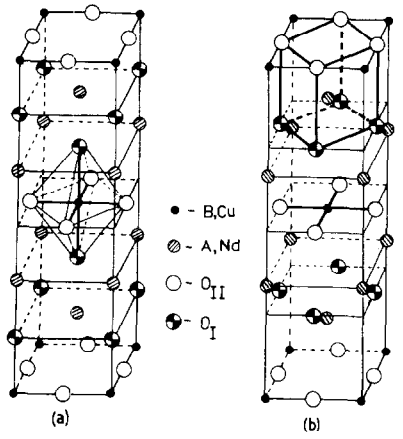

FIG. 1. Relation between (a) the K_2NiF_4 structure of tetragonal-T A_2BO_4 oxides and (b) the tetragonal-T' Nd_2CuO_4 structure.

calized $3d^1_{z^2}$ level by the conduction-band edge. In view of the stability of the $Cu^+ : 3d^{10}$ configuration, such a model is quite unrealistic. Goodenough (*7*) suggested an alternate configuration change within the $3d$-state manifold: $d^2_{z^2}\sigma^{*1}_{x^2-y^2} \rightarrow d^1_{z^2}\sigma^{*2}_{x^2-y^2}$, where the $d_{x^2-y^2}$ orbitals are broadened into a narrow $\sigma^*_{x^2-y^2}$ band by strong Cu—O—Cu interactions within the basal planes of La_2CuO_4. His model was based on the incorrect assumption that the tetragonal Pr_2CuO_4 phase has the K_2NiF_4 structure. As a result of the availability of considerably more structural, transport, and magnetic data, we suggest a more subtle configuration change in the present paper.

The correct structure of the tetragonal Pr_2CuO_4 phase was first determined for Nd_2CuO_4 by Müller-Buschbaum and Wollschlager (*8*); it is compared with the tetragonal K_2NiF_4 structure in Fig. 1. The cations and the O_{II} atoms shared by the transition-metal (B) cations are in identical positions in the two structures. The remaining O_I atoms have five A-cation and one B-cation nearest neighbors in the tetragonal (T) K_2NiF_4 structure; they are shifted in the tetragonal (T') Nd_2CuO_4 structure to tetrahedral interstices of the A-cation bilayers. Both tetragonal structures belong to space group *I4/mmm*.

The correct structure for the tetragonal-T' phase accounts well for the sharp increase in volume that accompanies the drop in c/a ratio and metal–semiconductor transition as the structure changes from orthorhombic (O) to tetragonal-T' with composition in the systems $La_{2-x}Ln_xCuO_4$ (*9, 22*).

The distortion to orthorhombic symmetry may have one or two components. One component has been identified in Sm_2CoO_4, the other in La_2CoO_4 (*10*). In Sm_2CoO_4, cooperative atomic displacements of the Sm(A) cations and the O_I atoms along the *c*-axis, see Fig. 2a, create two distinguishable A cations, Sm_I and Sm_{II}, as well as two distinguishable B cations, Co_I and Co_{II}. The displacements reduce the electrostatic repulsions between half the A cations and reduce every A—O_I bond length parallel to the *c*-axis. The Co—O_I bond lengths along the *c*-axis are different for Co_I and Co_{II} atoms. Along the orthorhombic *b*-axis, the A—O_I—A angle is reduced from 180°; along the *a*-axis it remains nearly 180°. Therefore the *b*-axis decreases while the *a*-

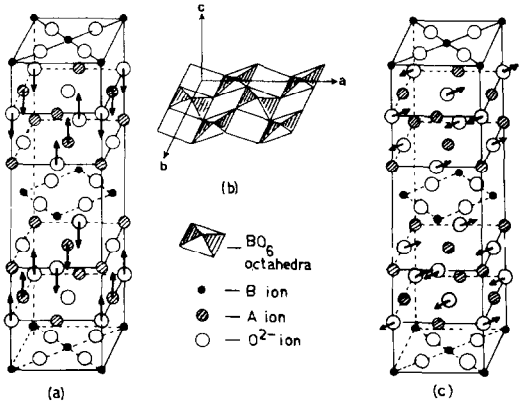

FIG. 2. Proposed atomic displacements for (a) the orthorhombic C^{18}_{2v}-*Fmm*2 structure of Sm_2CoO_4, (b) the added component in the orthorhombic D^{18}_{2h}-*Cmca* structure of La_2CoO_4, and (c) the monoclinic structure of Pr_2NiO_4.

axis remains essentially constant. Such a relationship between the a and b axes of this orthorhombic phase, space group C_{2v}^{18}-$Fmm2$, has been nicely demonstrated in the system $Ca_{1+x}Y_{1-x}CrO_4$, which exhibits an orthorhombic-tetragonal phase change with increasing temperature (*11, 12*). The three phases of $CaYCrO_4$ are particularly instructive as the structure shows an evolution with increasing temperature from an orthorhombic phase with two components below 840°C, to the orthorhombic phase with only the one component of Sm_2CoO_4 in the interval 800°C $< T <$ 1400°C, and a second transition to the tetragonal-T phase above 1400°C (*12*). The second component is represented by La_2CoO_4, space group D_{2h}^{18}-$Cmca$ (or $Abma$), which has been refined (*10*) in terms of a rotation of the CoO_6 octahedra about the orthorhombic b-axis (see Fig. 2b). Such a rotation shortens the a-axis while leaving the b-axis unchanged. The temperature variation of the lattice parameters of $CaYCrO_4$ (*12*) can be interpreted as follows: only the orthorhombic distortion represented by Fig. 2a is present in the temperature interval 840°C $< T <$ 1400°C, so the b-axis decreases with decreasing temperature while the a-axis remains constant; below 840°C, the O_{II} atoms move in the sense of the rotations of Fig. 2b to superpose an additional distortive component, so the a-axis decreases with decreasing temperature from 840°C while the b-axis changes relatively little. At room temperature the magnitudes of the a and b axes approach each other, so that a transition at lower temperatures to a tetragonal (T″) phase can be anticipated in which the unit-cell basal plane has double the area of that of the tetragonal T and T′ phases.

Determination of the orthorhombic phase of La_2CuO_4 was done on a single crystal prepared at high temperatures (*13*); the X-ray spectrum was refined in space group D_{2h}^{18}-$Abma$ ($Cmca$) on the basis of only the rotational component of Fig. 2b. Undoubtedly both components were present, especially as powder data taken on samples prepared at much lower temperatures and with controlled stoichiometry exhibit the $(h + k) = 2n$, $(k + l) = 2n$, and $(l + h) = 2n$ reflections consistent with space group C_{2v}^{18}-$Fmm2$ (or Fmm) rather than only the $h + k = 2n$ reflections of D_{2h}^{18}-$Cmca$. We conclude that stoichiometric, orthorhombic La_2CuO_4 contains primarily, if not exclusively, the distortive component represented by Fig. 2a. The O $\rightleftharpoons$ T transition, which is second order, should not be confused with the first-order O $\rightleftharpoons$ T′ transition encountered with compositional variation x in the systems $La_{2-x}Ln_xCuO_4$.

Low-temperature magnetic-susceptibility measurements on La_2CuO_4 have indicated the presence of a localized-moment contribution corresponding to about 0.5 μ_B per mole of La_2CuO_4 (*14*). This observation must be reconciled with the metallic character of La_2CuO_4. The existence of a localized-moment component has been confirmed in a sample exhibiting an ESR signal ($g_\parallel = 3.04$ and $g_\perp \simeq 2.06$), and it was interpreted to represent a Cu^{2+}-ion moment at a concentration of about 3.5 mole% associated with a magnetic impurity of a copper-containing second phase even though no evidence of a second phase was found in the powder X-ray diffraction data (*15*). In this paper we argue that the localized moments are an intrinsic property of La_2CuO_4.

On the other hand, the tetragonal-T′ phases Ln_2CuO_4 with Ln = Pr, Nd, or Gd—although semiconducting—exhibit a magnetic susceptibility below 300 K that is entirely due to the rare-earth ions decoupled from any antiferromagnetic order that may be present among the Cu—O_{II}—Cu layers (*16, 23*). This observation must be reconciled with any model that is proposed for the Ln_2CuO_4 phases.

In the Ni(II) oxides, structural refinement (*17*) of La_2NiO_4 has confirmed the tetragonal-T structure and determined an

TABLE I

CRYSTAL STRUCTURE AND LATTICE PARAMETERS OF THE SYSTEMS $La_2Ni_{1-x}Cu_xO_4$, $La_{2-2x}Sr_{2x}Ni_{1-x}Ti_xO_4$, $Pr_2Ni_{1-x}Cu_xO_4$, $La_{2-x}Pr_xCuO_4$, AND $La_{2-x}Nd_xCuO_4$

Compound	Crystal[a] structure	Lattice parameters (Å)		
		a	*b*	*c*
$La_2Ni_{1-x}Cu_xO_4$				
$x = 0.0$	T	3.85	—	12.65
0.25	T	3.84	—	12.76
0.50	T	3.82	—	12.93
0.75	T	3.81	—	13.05
0.90	O	5.37 (3.804)[b]	5.39	13.13
1.00	O	5.36	5.41	13.17
$Pr_2Ni_{1-x}Cu_xO_4$				
$x = 0.0$[c]	M	3.841	3.853	12.44
0.10[c]	M	3.832	3.837	12.486
0.25	T	3.83	—	12.56
0.50	T	3.83	—	12.60
0.75	T and T′			
0.90	T′	3.96	—	12.22
1.00	T′	3.96	—	12.18
$La_{2-2x}Sr_{2x}Ni_{1-x}Ti_xO_4$				
$x = 0.25$	T	3.86	—	12.67
0.50	T	3.87	—	12.67
0.75	T	3.87	—	12.63
1.00	T	3.88	—	12.60
$La_{2-x}Pr_xCuO_4$[d]				
$x = 0.25$	O	5.357 (3.804)[b]	5.404	13.13
0.50	O	5.357 (3.804)[b]	5.402	13.10
0.75	T′	3.976	—	12.56
1.25	T′	3.966	—	12.43
1.75	T′	3.962	—	12.38
2.00	T′	3.958	—	12.28
$La_{2-x}Nd_xCuO_4$[d]				
$x = 0.10$	O	5.356 (3.804)[b]	5.402	13.15
0.25	T′	3.975	—	12.32
0.50	T′	3.975	—	12.30
1.50	T′	3.961	—	12.27
1.75	T′	3.957	—	12.22
2.00	T′	3.945	—	12.17

[a] T, tetragonal K_2NiF_4 structure; T′, tetragonal Nd_2CuO_4 structure; O, orthorhombic structure; M, monoclinic structure. See text for more details.

[b] Pseudo-tetragonal *a* parameter.

[c] $\gamma = 90.30°$ for $x = 0.0$ and $90.30°$ for $x = 0.10$.

[d] Data reported earlier in Ref. (*22*).

La—O_I bond length parallel to the *c*-axis of only 2.32 Å compared to the 2.62 Å predicted from the Shannon–Prewitt (*18*) ionic radii. The structure of Pr_2NiO_4, on the other hand, is monoclinic (M) (see Table I). This monoclinic phase is to be distinguished from that reported previously (*36*); it is not indexable on an orthorhombic cell as it creates distinguishable Ni—O_{II}—Ni distances. It can be generated by an antiferroelectric displacement of the O_I ions of a bilayer along [100] and [$\bar{1}$00] directions of the T phase as illustrated in Fig. 2c.

The magnetic susceptibility of La_2NiO_4 exhibits a Curie–Weiss law above 200 K, and an inflection at 200 K was attributed to the appearance at lower temperature of a weak ferromagnetism due to a Dzialoshinskii spin canting of an antiferromagnetically ordered system (*19*). However, neither a subsequent neutron-diffraction study (*20*) nor magnetic-susceptibility data (*23*) provide any evidence of antiferromagnetic order at lowest temperatures. In this paper we reinvestigate the low-temperature susceptibility in the systems $La_2Ni_{1-x}Cu_xO_4$ and $La_{2-2x}Sr_{2x}Ni_{1-x}Ti_xO_4$ to show that there is a reduction of the nickel magnetic moment below the inflection temperature. This finding is discussed in terms of an energy diagram proposed earlier (*7*) and on the subsequent emphasis on the evidence for a coexistence of localized and itinerant 3*d* electrons in La_2NiO_4 as a result of the anisotropic character of the structure (*21*).

The structural and conductivity data for the mixed systems $(La,Ln)_2CuO_4$ (*Ln* = Pr, Nd) and $La_2(Cu,Ni)O_4$ (*22*) as well as the magnetic data for Ln_2CuO_4 and Ln_2NiO_4 (*Ln* = La, Pr, Nd) (*23*) have been reported previously. In this paper we report the variations in the lattice parameters of these systems and some ir and ESR data in addition to some new magnetic and transport data. We comment on the relationship between the various phases that are encountered, and we discuss the physical properties in terms of the energy-band diagrams for the Cu(II) and Ni(II) systems. In particular, we note that a K_2NiF_4 structure with tolerance factor $t < 1$ imposes a pressure contracting the B—O_{II} bond lengths in the basal plane, and we argue that this pressure produces some extraordinary properties wherever

the $d_{x^2-y^2}$ orbitals may be thereby transformed in character from localized to itinerant.

Experimental

A. Preparation

The $La_2Ni_{1-x}Cu_xO_4$ samples were identical to those for which the electrical properties have already been reported (*22*). The $Pr_2Ni_{1-x}Cu_xO_4$ samples were prepared similarly, but with a final firing temperature of 1370 K.

The $La_{2-2x}Sr_{2x}Ni_{1-x}Ti_xO_4$ compounds were prepared by thoroughly mixing and grinding under alcohol for several hours stoichiometric mixtures of $La_2(C_2O_4)_3 \cdot nH_2O$ (n determined thermogravimetrically), $SrC_2O_4 \cdot H_2O$, $NiC_2O_4 \cdot 2H_2O$, and TiO_2. The mixture was decomposed in air by slowly heating to 1270 K; the product was then heated at 1570 K for 72 hr with intermittent grinding and pelletizing.

The $La_{2-x}Ln_xCuO_4$ (Ln = Pr, Nd) samples were coprecipitated from solutions of the corresponding metal chlorides made up in the required proportions. The mixture of chlorides was added slowly to a fairly concentrated solution of Na_2CO_3 with constant stirring, and the precipitated carbonate was washed to remove any excess Na_2CO_3. The precipitate was then decomposed and sintered at 1270 K for 48 hr with intermittent grinding and pelletizing repeated several times.

B. X-Ray Diffraction

Temperature-dependent X-ray diffraction data were taken with a Philips-PW 1050/70 diffractometer and Ni-filtered Cu$K\alpha$ radiation. The data were collected at a scan rate of 1/4° per minute.

The room-temperature lattice parameters and c/a ratio for different values of x in the systems $La_2Ni_{1-x}Cu_xO_4$ and $La_{2-2x}Sr_{2x}Ni_{1-x}Ti_xO_4$ are given in Table I. Végard's law is obeyed for both systems, which indicates the formation of true solid solutions. Neither the X-ray nor the electron diffraction spectra showed any evidence of a superstructure in $La_{2-2x}Sr_{2x}Ni_{1-x}Ti_xO_4$, even for $x = 0.5$, so the Ni^{2+} and Ti^{4+} ions appear to be randomly distributed. It is to be noted that the mean Ni—O and Cu—O distances, averaged over all six nearest oxide-ion neighbors, are 2.02 and 2.07 Å, respectively, in La_2NiO_4 (*2*) and La_2CuO_4 (*4*); these are significantly smaller than the 2.09 and 2.13 Å distances calculated from the Shannon–Prewitt ionic radii.

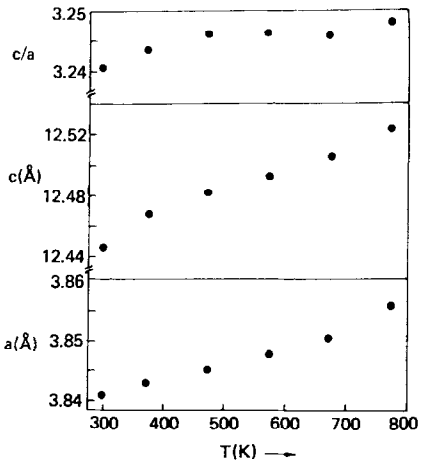

FIG. 3. Temperature dependence of the lattice parameters of Pr_2NiO_4.

Table I also gives the room-temperature structural data for several compositions in the systems $La_{2-x}Ln_xCuO_4$ with Ln = Pr or Nd and $Pr_2Ni_{1-x}Cu_xO_4$. A structural change from orthorhombic to tetragonal-T′ is apparent for the $La_{2-x}Ln_xCuO_4$ systems at critical concentrations x_c, where $0.5 < x_c < 0.75$ for Ln = Pr and $0.10 < x_c < 0.25$ for Ln = Nd. A change from monoclinic-M to tetragonal-T also occurs in $Pr_2Ni_{1-x}Cu_xO_4$ at an x_c in the range $0.1 < x_c < 0.25$; the $x = 0.75$ sample contains T and T′ phases, and the T′ phase is stabilized for $x > 0.9$.

The c/a ratio of La_2NiO_4 increases with increasing temperature (*21*); and a similar,

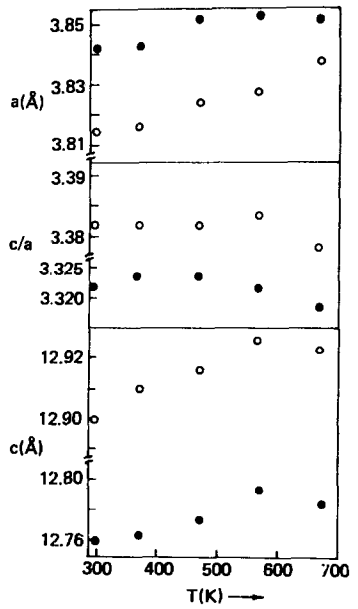

FIG. 4. Temperature dependence of the lattice parameters of $La_2Ni_{1-x}Cu_xO_4$, $x = 0.25$ (●) and 0.5 (○).

smaller increase was observed in Pr_2NiO_4 (Fig. 3), which undergoes a smooth monoclinic–tetragonal transition at $T_t \simeq 670$ K. However, samples with $x = 0.25$ and 0.5 in the system $La_2Ni_{1-x}Cu_xO_4$ showed little temperature variation of the c/a ratio (see Fig. 4).

C. Magnetic Susceptibility

Magnetic susceptibilities were obtained with a Faraday balance and a Cahn RG vacuum, recording electrobalance. A closed-cycle helium-refrigeration system gave a lower limit of 12 K to the temperature range; the upper limit was 1000 K. $HgCo(SCN)_4$ was used as a calibrant, and the susceptibility was measured at various fields up to 5000 G. All samples but La_2CuO_4 had field-independent susceptibilities; extrapolation to $H = 0$ of the weak field dependence of La_2CuO_4 permitted determination of a weak ferromagnetic component below about 850 K. The field dependence was also found in La_2CuO_4 samples

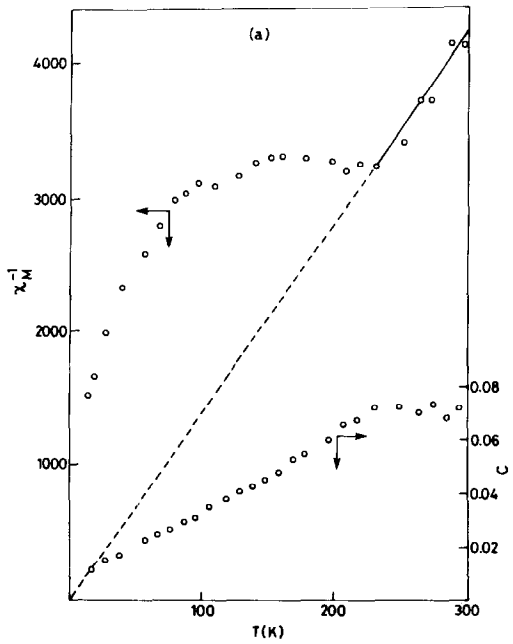

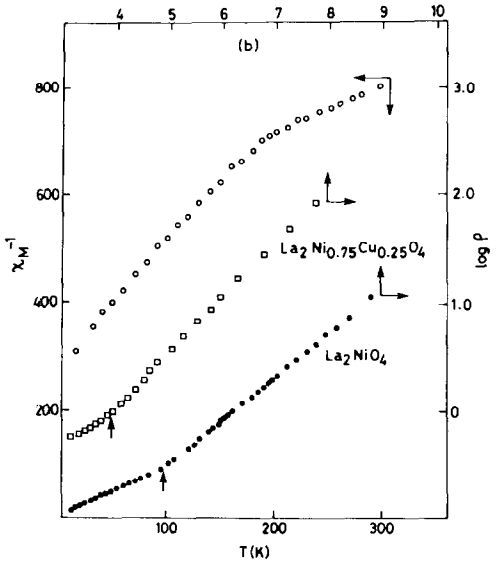

FIG. 5. Temperature dependence of molar magnetic susceptibility χ_m and resistivity ρ for $La_2Ni_{1-x}Cu_xO_4$, $x = 0.0$, 0.25, and 1.0: (a) χ_m^{-1} vs T plot of La_2CuO_4 (without contribution from ferromagnetic impurity) and variation of Curie constant C based on a Curie law for all T; (b) χ_m^{-1} vs T of La_2NiO_4 and log ρ vs T^{-1} of La_2NiO_4 and $La_2Ni_{0.75}Cu_{0.25}O_4$.

prepared from oxides of high purity by a ceramic method. Mehran and Machin (*24*) have reported a similar weak ferromagnetism in several oxides of copper whereas Saez Puche *et al.* (*15*) report no field dependence of the susceptibility of their sample of La_2CuO_4. We therefore presume that the ferromagnetism is not intrinsic to La_2CuO_4. This component saturates to a constant value of about 0.004 μ_B/mole below 300 K, and the paramagnetic susceptibility of La_2CuO_4 shown in Fig. 5a was obtained from the slope of the straight-line portion of the M vs H plots at higher values of H.

In agreement with earlier work (*19*), the magnetic susceptibility of La_2NiO_4 was found to obey a Curie–Weiss law above 200 K with a Weiss constant $\theta = -500$ K and a $\mu_{eff} \simeq 3.03\ \mu_B$ per Ni^{2+} ion, which is higher than the spin-only value of 2.83 μ_B for an $S = 1$ system. However, a $g \simeq 2.12$ may be inferred for octahedral Ni^{2+} ions from the magnetization of the spinel $Fe^{3+}[Ni^{2+}Fe^{3+}]O_4$ (*39*).

As can be seen in Fig. 5b, the inverse molar susceptibility χ_m^{-1} versus temperature T has an inflection at $T_d \simeq 200$ K, where we define T_d as the inflection (or deflection) temperature. It is to be noted that below T_d, the magnetic susceptibility obeys a different Curie–Weiss law with a slope for χ_m^{-1} vs T corresponding to a $\mu_{eff} = 1.83\ \mu_B$, which is close to the spin-only value of 1.73 μ_B for an $S = 1/2$ system. Moreover, the Weiss constant $\theta \simeq -120$ K is only a little smaller than would be deduced from the change in Curie constant $C \simeq \mu_{eff}^2/8$ and the relation $\theta = CW$ for a constant Weiss molecular-field parameter W. Yet there is no evidence of any long-range order down to 12 K, which is consistent with the neutron-diffraction data (*20*).

Table II shows the parameters C, μ_{eff}, and θ obtained above and below a T_d in the systems $La_{2-2x}Sr_{2x}Ni_{1-x}Ti_xO_4$ and $La_2Ni_{1-x}Cu_xO_4$. The temperature T_d is not so sharply defined in the mixed systems; but as can be seen from Figs. 5b and 6 for the $La_2Ni_{1-x}Cu_xO_4$ system, the slope of the low-temperature inverse magnetic susceptibility gives a nearly constant μ_{eff} per Ni^{2+} atom for $x < 0.5$; only the magnitude of the Weiss constant θ decreases. However, in the $x = 0.75$ sample there is evidence of a contribution to the susceptibility from the Cu^{2+} ions. For all x, the high-temperature data remains consistent with a contribution from only the Ni^{2+} ions having, for $T > T_d$, a spin $S = 1$ (see Table II).

In the systems $La_{2-x}Pr_xCuO_4$ and $La_{2-x}Nd_xCuO_4$, the magnetic susceptibility obeyed a Curie–Weiss law that was completely dominated by the rare-earth ion in both the O and T′ phases.

D. Electrical Resistivity

The electrical resistivity of La_2CuO_4 has a nearly temperature-independent resistivity of about 0.1 ohm-cm above 200 K except for a small maximum near 530 K that is associated with a smooth O $\rightleftharpoons$ T transition at this temperature (*5*). The room-temperature Seebeck coefficient $\alpha = 200\ \mu V/K$ is large, positive, and apparently temperature-independent. The low-temperature ($T < 200$ K) resistivity, on the other hand, shows a marked increase with decreasing temperature; the ratio of the resistivities at 14 and 200 K is about 10^2 (see Fig. 7).

The orthorhombic solid solutions $La_{2-x}Pr_xCuO_4$, $0 < x < 0.5 < x_c$, also exhibit a nearly temperature-independent resistivity at high temperatures except for a small maximum near T_t for the O $\rightleftharpoons$ T transition, which shifts to higher temperature with increasing x (*22*); and at low T they show the same sharp increase in resistivity as found in La_2CuO_4, but with an onset temperature that shifts to lower temperature with increasing x (see Fig. 8).

The electrical resistivity of La_2NiO_4 can be separated into three distinct temperature intervals. A shallow minimum of about 3 ×

TABLE II

MAGNETIC SUSCEPTIBILITY AND ELECTRICAL RESISTIVITY DATA OF $La_2Ni_{1-x}Cu_xO_4$ AND $La_{2-2x}Sr_{2x}Ni_{1-x}Ti_xO_4$

Compound	Magnetic susceptibility data[a] C (emu,K/mole)	μ_{eff} (μ_B)	θ (K)	T_d[b] (K)	T_{min}[c] (K)	E_a[d] (eV)
$La_{2-2x}Sr_{2x}Ni_{1-x}Ti_xO_4$						
$x = 0.0$	1.15	3.03	500	200	620	0.053
	(0.42)	(1.83)	117			(0.081)
0.25	1.09	2.96	430	240		0.083
0.50	1.05	2.90	300			
0.75	0.93	2.73	0			0.136
$La_2Ni_{1-x}Cu_xO_4$						
$x = 0.25$	1.11	2.98	380	240	660	0.087
	(0.43)	(1.86)	(42)			(0.104)
0.50	1.02	2.86	270	280	735	0.107
	(0.40)	(1.79)	(10)			
0.75	0.99	2.82	200	310	800	0.110
	(0.57)	(2.14)	(27)			

[a] C and μ_{eff} are calculated per gram-atom of Ni. Figures in brackets refer to data below 100 K, all others are obtained from data above 300 K.

[b] T_d obtained from susceptibility data and refers to the temperature at which there is deviation from the high-temperature Curie–Weiss law.

[c] T_{min} is the temperature at which the resistivity shows a minimum. The electrical resistivity behavior is reported elsewhere (*22*).

[d] Activation energy obtained from data ($T > 300$ K) reported in Ref. (*22*). Figures in brackets refer to E_a for $T < T_d$.

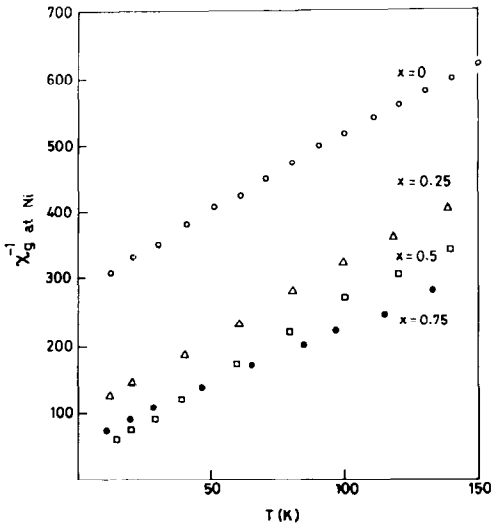

FIG. 6. Temperature dependence of susceptibilities of samples from the systems $La_2Ni_{1-x}Cu_xO_4$ ($T < 150$ K) calculated per gram-atom of Ni.

10^{-2} ohm-cm occurring at $T_{min} \simeq 600$ K makes the compound metallic-like for $T > T_{min}$ and semiconducting for $T < T_{min}$. The log ρ versus T^{-1} plot shows a break in the slope at $T_d \simeq 200$ K; the activation energy E_a defined by $\rho = \rho_0 \exp(-E_a/kT)$ changes from 0.082 eV for $T < T_d$ to 0.053 eV for $T > T_d$ (see Fig. 5b).

It is of interest to note that for $T > T_d$, the relation $E_a \simeq kT_{min}$ holds in La_2NiO_4. Such a relation is also found in the system $Pr_2Ni_{1-x}Cu_xO_4$, Table II and Fig. 9a, and in Nd_2NiO_4 (*25*), which exhibit a similar resistivity minimum at high temperatures. An $E_a > 0.82$ eV would make $E_a/k > 1000$ K, which is beyond the range of our measurements; accordingly no resistivity minimum was observed for samples $x = 0.25$ and 0.5 of the system $La_{2-2x}Sr_{2x}Ni_{1-x}Ti_xO_4$ (see Fig. 9b).

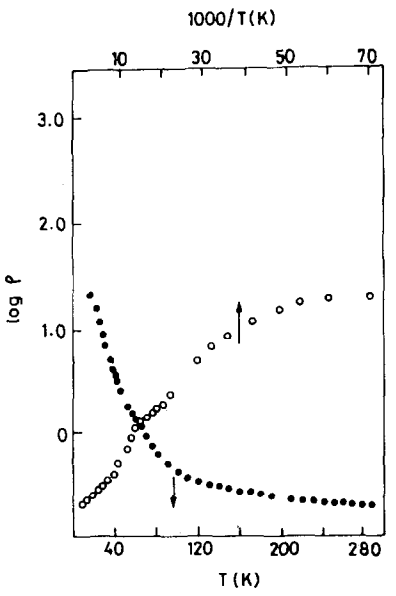

FIG. 7. Temperature dependence of electrical resistivity ρ in ohm-cm of La_2CuO_4: log ρ vs T and log ρ vs T^{-1}.

On the other hand, in the system $La_2Ni_{1-x}Cu_xO_4$ the relation $E_a = kT_{min}$ was not obeyed for $x \neq 0$, see Table II. In this system the break at T_d is still well-marked in the $x = 0.25$ sample, see Fig. 5b, but for higher values of x the definition of T_d becomes blurred.

E. Infrared Studies

The ir spectra in the range 800–300 cm^{-1} are shown in Fig. 10 for La_2NiO_4 and Ln_2CuO_4 (Ln = La, Pr, Nd, and Sm). They were taken with a Perkin–Elmer 580 spectrophotometer. The temperature-dependent ir spectra for $La_2Ni_{0.75}Cu_{0.25}O_4$ (Fig. 11) and Nd_2CuO_4 (Fig. 12) were obtained with a temperature-controlled Specac variable-temperature cell. The samples were mixed thoroughly with dry KBr (concentration of sample about 1 wt%) and pressed into disks of about 0.5-mm thickness.

The strong absorption band around 680 cm^{-1} for orthorhombic La_2CuO_4 is not present in the T′ phases of the other Ln_2CuO_4 compounds (see Fig. 10). Since the difference in the two structures is a change in the O_I-atom position from a linear La—O_I—Cu linkage along the c-axis in the O phase to a tetrahedral interstice of the Ln_2 bilayers in the T′ phase, the absorption may be assigned to the very short La—O_I bond in La_2CuO_4; it has a length of 2.40 Å compared to an average La—O separation of 2.60 Å (*4*). The other two bands of the La_2CuO_4 spectrum may be assigned to asymmetric stretching and bending modes of the strong Cu—O_{II} linkages in the basal planes.

The tetragonal-T phase of La_2NiO_4 has a short La—O_I bond parallel to the c-axis analogous to that in La_2CuO_4, and all the $La_2Ni_{1-x}Cu_xO_4$ compounds give spectra similar to that of La_2CuO_4. The band assigned to the short La—O_I distance shifts to higher energies with increasing copper content.

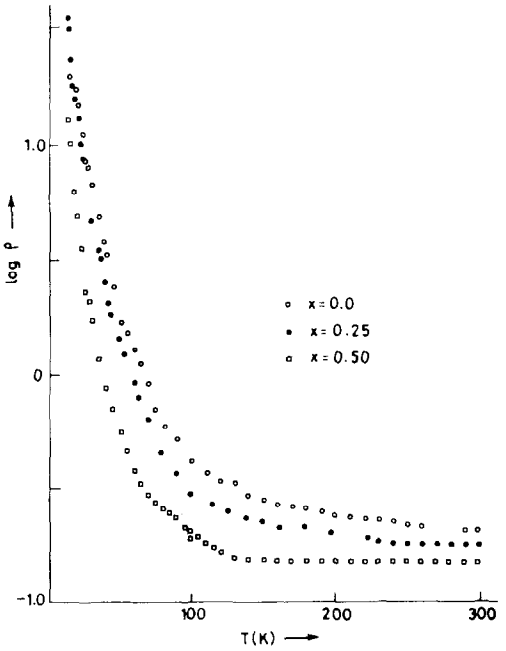

FIG. 8. Temperature dependence of electrical resistivity ρ in ohm-cm for $La_{2-x}Pr_xCuO_4$ with x = 0.0, 0.25, and 0.50.

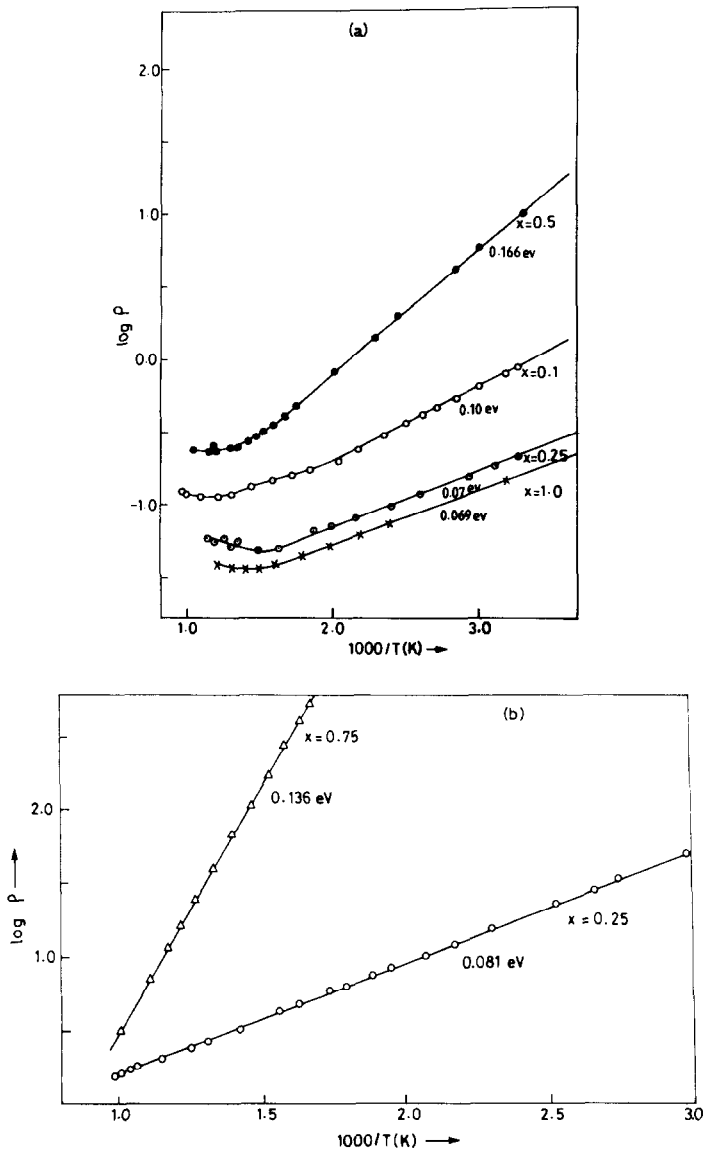

FIG. 9. Temperature dependence of electrical resistivity ρ in ohm-cm for (a) $Pr_2Ni_{1-x}Cu_xO_4$ and (b) $La_{2-2x}Ni_{1-x}Ti_xO_4$.

Figure 11 shows that, for the $x = 0.25$ sample, the frequency of the absorption band assigned to the La—O_I stretch increases with decreasing temperature, as expected for a stretching mode; it is consistent with the usual lattice-parameter contraction in a solid with the lowering of temperature. On the other hand, the frequency of the other band remains essentially temperature-independent, which is consistent with a bond under great internal pressure. In Nd_2CuO_4, which has the T′ phase and no such pressure on the Cu—O_{II} bond, the frequency of the absorption band increases with decreasing temperature in the usual way (see Fig. 12).

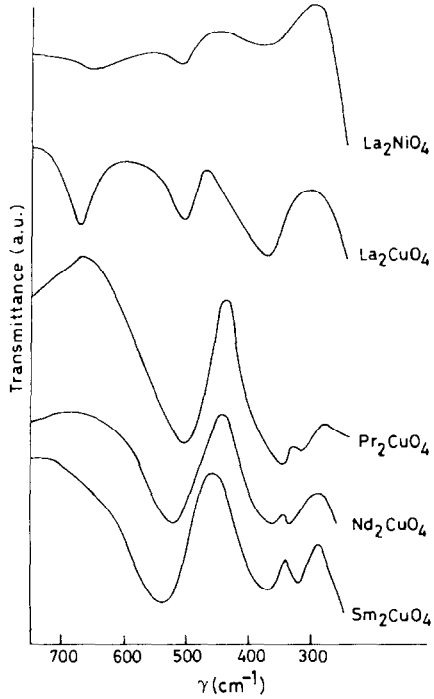

FIG. 10. Infrared spectra of La_2NiO_4 and Ln_2CuO_4 (Ln = La, Pr, Nd, and Sm).

F. ESR Study

Room-temperature ESR spectra for powdered specimens in magnetic fields ranging from 0 to 8 kG were recorded on a Varian E-109 spectrometer. Spectra of the $La_{2-x}Pr_xCuO_4$ system are shown in Fig. 13. The important features are

(i) La_2CuO_4 shows no ESR signal, contrary to the sample of Saez Puche *et al.* (*15*).

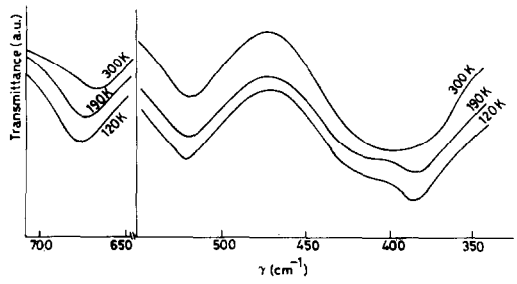

FIG. 11. Temperature dependence of infrared spectrum of $La_2Ni_{0.75}Cu_{0.25}O_4$.

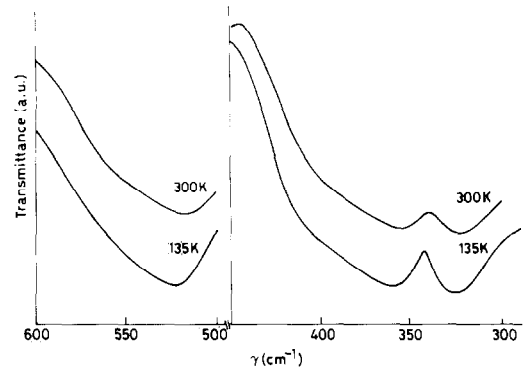

FIG. 12. Temperature dependence of infrared spectrum of Nd_2CuO_4.

(ii) Orthorhombic samples containing Pr gave a fairly isotropic signal with a $g \simeq 2.2$ (curves B and C).

(iii) The $x = 0.75$ sample, curve D, gives a signal typical of a superposition on the isotropic signal of a signal from a square-coplanar coordination.

(iv) The $x = 1.75$ sample, curve E, and pure Pr_2CuO_4, curves F and G (140 K), are entirely different. They indicate an axial S

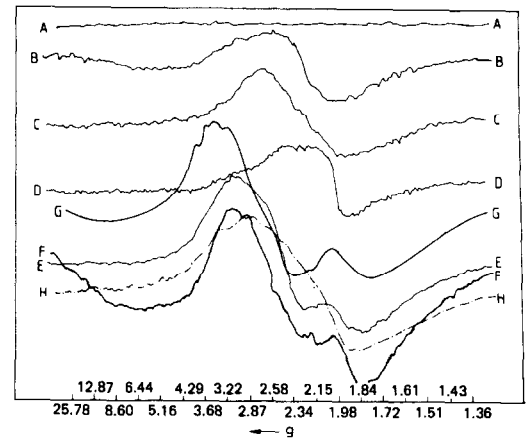

FIG. 13. Room-temperature X-band (9.04 GHz) ESR spectrum of $La_{2-x}Pr_xCuO_4$: (A) $x = 0.0$, (B) $x = 0.25$, (C) $x = 0.50$, (D) $x = 0.75$, (E) $x = 1.75$, (F) $x = 2.00$, (G) $x = 2.00$ (147 K); and of Sm_2CuO_4 (H).

= 1/2 ground state typical of Cu^{2+} ions in compressed octahedra (*26*) or in elongated octahedra with antiferrodistortive ordering (*37*).

(v) The ESR spectrum of Sm_2CuO_4, curve H, is again different. It is compatible with the behavior expected from exchange coupling between axial $S = 1/2$ ground states of Cu^{2+} ions in compressed octahedra (*26*).

The systematics of these changes would seem to rule out the possibility that the ESR signals are due to copper ions in impurity phases. The absence of any localized-moment contribution from the copper to the magnetic susceptibility therefore suggests that the ESR signals are associated with an electron in an oxygen vacancy or other defect.

Discussion

A. Structural Considerations

It is useful to define a tolerance factor

$$t = R_{AO}/\sqrt{2}\,R_{BO} \qquad (1)$$

for the tetragonal-T phase; R_{AO} and R_{BO} are the sums of the ionic radii for A or B cations and the oxide ion (*27*). Empirically, distortions from tetragonal symmetry are found where the tolerance factor is $t < 0.87$. They may also occur for $0.87 < t < 1$ in certain cases.

If a T phase has $t < 1$, geometry imposes the following constraint: in the basal planes, the B—O_{II}—B distance is shortened and the A—O_I—A distance is lengthened relative to $2R_{BO}$ and $2R_{AO}$. In other words, the A—O_I—A bonding, which is stretched, applies pressure on the B—O_{II}—B bonds. Because of the asymmetric potential function, shortening of the B—O_{II}—B bonds tends to be less than the stretching of the A—O_I—A bonds despite there being double the number of bonds in an A—O_I bilayer relative to a B—O_{II} monolayer. Nevertheless, the in-plane pressure on the B—O_{II} bonds is large as t approaches the limiting value of $t \simeq 0.87$. This fact is of critical importance for the energy-band models to be proposed.

In addition, each cation will adjust the c-axis A—O_I and B—O_I bond lengths so as to balance the mean M—O distance of its nearest neighbors, which means that the c-axis A—O_I bond lengths are shortened and the B—O_I bond lengths are lengthened. At a transition-metal B cation, the d_{z^2} orbitals are stabilized relative to the $d_{x^2-y^2}$ orbitals and the $d_{yz}d_{zx}$ orbitals are stabilized relative to the d_{xy} orbitals. This fact is manifest in significantly larger axial ratios c/a if the B cation is a Jahn-Teller ion such as high-spin Mn^{3+}, low-spin Ni^{III}, or Cu^{2+}, which have E_g ground states in octahedral symmetry.

The c-axis A—O_I and B—O_I bond lengths are also influenced by two other factors: (i) the relative strengths of the A—O_I and B—O_I bonding in an A—O_I—B linkage and (ii) the A—A electrostatic repulsion between c-axis near neighbors (see Fig. 1). In compounds with trivalent A cations and divalent B cations, the A—O_I interaction competes favorably with the B—O_I interaction along the c-axis, and the B—O_I bond lengths are longer than B—O_{II} bond lengths.

The tolerance factor for La_2NiO_4 is $t \simeq 0.89$, so the Ni—O_{II} bond length in the basal plane is reduced to 1.93 Å, significantly shorter than the $R_{NiO} = 2.09$ Å obtained from the Shannon–Prewitt radii. This produces an unusually strong Ni: $d_{x^2-y^2}$—O_{II} : p_σ—Ni : $d_{x^2-y^2}$ interaction. In view of the high Néel temperature in NiO, which shows that the Ni : e_g—O : p_σ—Ni : e_g interactions approach the limit where the super exchange perturbation expansion breaks down even with normal bond lengths, it is at once apparent that the $d_{x^2-y^2}$ orbitals must be represented by a narrow $\sigma^*_{x^2-y^2}$ band of itinerant-electron states (*7, 28*). The only issue to be resolved experimentally is the strength of the correlations

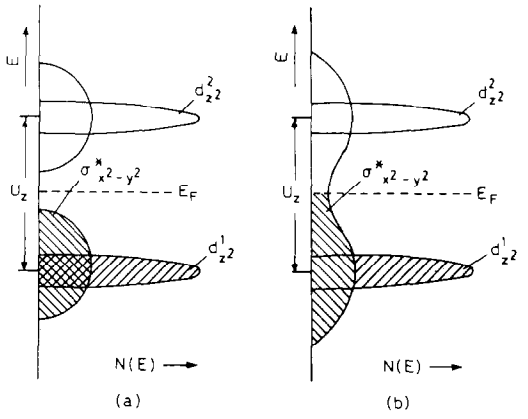

FIG. 14. Schematic density of states vs energy diagrams for the σ-bonding $3d$ electrons of La_2NiO_4. U_z is the correlation splitting of $d^1_{z^2}$ and $d^2_{z^2}$ levels. Not shown are filled $O^{2-}: 2p^6$ and $Ni^{2+}: t^6_{2g}$ bands, empty Ni^{2+} $4s$ and La^{3+} : $6s$ and $5d$ bands. (a) $\sigma^*_{x^2-y^2}$ band split by either electron correlations or a charge-density wave, (b) no splitting of $\sigma^*_{x^2-y^2}$ band (after Ref. (*21*)).

in this narrow band. Since the Ni—O_I—La—□—La—O_I—Ni and Ni—O_I—O_I—Ni interactions are negligible or small and, from the geometry of the overlap integrals, the Ni : d_{z^2}—O_{II} : p_σ—Ni : d_{z^2} interaction is sharply reduced relative to the Ni : $d_{x^2-y^2}$—O_{II} : p_σ—Ni : $d_{x^2-y^2}$ interaction, the Ni : d_{z^2} orbitals are strongly correlated and can be considered localized in the sense that the Ni—O_{II}—Ni interaction can be described by a superexchange second-order perturbation theory. Since the $d^1_{z^2}$ energy is lower than the mean energy of the occupied states of the half-filled $\sigma^{*1}_{x^2-y^2}$ band and the $d^1_{z^2}$ configuration is split from the $d^2_{z^2}$ configuration by a correlation splitting approaching 3 eV, as determined for NiO (*29*), we obtain the schematic energy diagram shown in Fig. 14 (*21*). Since the Fermi energy E_F lies well above the $O^{2-}: 2p^6$ band edge (*29*), the nickel orbitals of t_{2g} parentage and the $O^{2-}: 2p^6$ bands need not be considered; similarly, the Ni : $4s$ band lies several eV from E_F, so it also is omitted from the diagram.

The tolerance factor for La_2CuO_4 is $t \simeq$ 0.87, but this departure from unity is considerably relieved (t_{eff} = 0.95 for R_{BO} = Cu—O distance in CuO) by an ordering of the σ-bonding $3d$ electrons into the configuration $Cu^{2+}: d^2_{z^2}\sigma^{*1}_{x^2-y^2}$ as previously suggested (see Fig. 15a) (*7*). However, it now appears that this energy diagram is only applicable to the T′-phase where the $d^2_{z^2}$ energy level is stabilized by removal of the O_I-atom near neighbors from the c-axis. In the T-phase, the $d^2_{z^2}$ levels probably do not fall completely below E_F, as will be argued in connection with the interpretation of the magnetic and transport data for La_2CuO_4 and the T $\rightleftharpoons$ O transition that occurs with increasing x in the system $La_2Ni_{1-x}Cu_xO_4$.

The orthorhombic distortion distinguishes two types of copper, each with a different Cu—O_I distance. Those with the longer Cu—O_I bond length have a more stable $d^2_{z^2}$ configuration; those with a shorter Cu—O_I bond length may have a $d^2_{z^2}$ configuration at an energy high enough to be intersected by E_F as illustrated in Fig. 15b. Such a situation would lead to physical properties analogous to those observed in the rare-earth compounds having "mixed configurations" (commonly referred to as intermediate valences) as a result of a

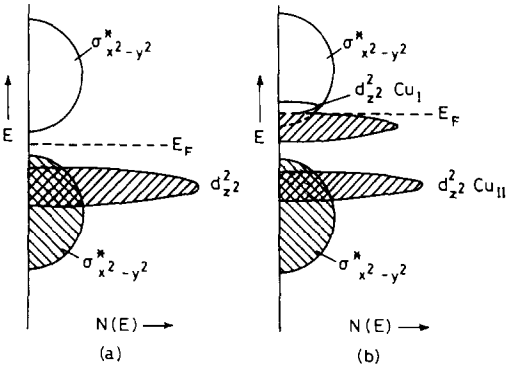

FIG. 15. Schematic density of states vs energy diagrams for the σ-bonding $3d$ electrons of (a) Pr_2CuO_4 with correlation splitting of the $\sigma^*_{x^2-y^2}$ band and (b) La_2CuO_4. Not shown are filled and empty bands as in Fig. 14.

Fermi energy of a partially filled conduction band intersecting a localized $4f^n$-configurational energy to create a $4f^{n+1}/4f^n$ couple. We will argue that the configuration change on going across the T′ ⇌ O transition is represented by the change from that of Fig. 15a with correlation splitting of the $\sigma^*_{x^2-y^2}$ band and a more normal Cu—O_{II} bond length to that of Fig. 15b with the anomalously short Cu—O_{II} bond lengths.

In cubic perovskites, distortions from cubic to orthorhombic symmetry selectively optimize some of the A—O bond lengths where a $t < 1$ stretches them in the cubic phase. In the tetragonal K_2NiF_4 structures under study, distortions to the orthorhombic structure appear to be stabilized by other factors besides a $t < 1$, which makes close correlation with a $t \simeq 0.87$ more difficult. In the system $Pr_2Ni_{1-x}Cu_xO_4$, the M ⇌ T transition (at $t \simeq 0.87$) with increasing x is consistent with the average tolerance factor t increasing with x as a result of the ordering of the Cu^{2+}: $3d^9$ electrons as $d^2_{z^2}\sigma^{*1}_{x^2-y^2}$. However, the T ⇌ O transition with increasing x in the system $La_2Ni_{1-x}Cu_xO_4$ does not then follow logically unless, in La_2CuO_4, there is an inability to stabilize $d^2_{z^2}$ configurations on all the Cu^{2+} ions in accordance with the energy diagram of Fig. 15a. A distortion to orthorhombic symmetry that distinguished two types of Cu^{2+} ions would tend to stabilize the $d^2_{z^2}$ configurations of half the Cu^{2+} ions (Fig. 15b), and it appears that the orthorhombic structure may be stabilized in La_2CuO_4 for this reason despite a $t_{eff} = 0.95$.

Stabilization of an orthorhombic distortion rather than a monoclinic-M or tetragonal-T′ distortion appears, empirically, to be associated with larger and more basic A cations. Although Pr_2CuO_4 has a tolerance factor $t \simeq 0.85$, the Cu—O distance of CuO gives a $t_{eff} = 0.91$. Nevertheless, the T′ phase is stabilized. Stabilization of this phase, which has an expanded basal plane allowing a Cu—O_{II} square-coplanar distance similar to that found in CuO, would seem to require (i) an A cation small enough to prevent stretching of a B—O_{II} bond length beyond R_{BO} and (ii) a reduced A—B electrostatic repulsion along the c-axis. Ordering of $d^2_{z^2}$ electrons along the c-axis at a Cu^{2+} ion provides an important screening of this latter repulsion, which accounts for the known stabilization of this phase exclusively with the Cu(II) oxides. The smaller size and greater acidity of the Pr^{3+} compared to the La^{3+} ion also favor the T′ phase in Pr_2CuO_4 relative to La_2CuO_4; and it is satisfying to note that the T′ phase is stabilized for the Ln_2CuO_4 compounds containing Ln = Pr to Gd with an x_c for the O ⇌ T′ transition in $La_{2-x}Ln_xCuO_4$ that is larger for Ln = Pr than for Ln = Nd (see Table I).

In Pr_2NiO_4 ($t = 0.86$), where there can be no reduction of the Pr^{3+}—Ni^{2+} electrostatic repulsion by ordering of electrons into d_{z^2} orbitals to form a $d^2_{z^2}$ configuration, the distortion is to monoclinic symmetry. This symmetry is compatible with a cooperative antiferroelectric displacement of O_I atoms along [100] and [$\bar{1}$00] directions of the T phase (see Fig. 2c), rather than a displacement through an A-cation face to a tetrahedral position as in the T′ phase. (The O_{II} atom may also be displaced slightly in the direction of a cooperative rotation about the [010] axis.) Such a displacement of the O_I atom reduces the length of the c-axis and allows stronger A—O_I bonding without removing all screening of the A—B electrostatic repulsion. The Ni—O_{II} bond length appears to be little changed by the T ⇌ M distortion, so the $\sigma^*_{x^2-y^2}$ bandwidth should not be significantly reduced on traversing this smooth transition. Similarly, little change in the $\sigma^*_{x^2-y^2}$ bandwidth will occur at a smooth O ⇌ T transition; but the situation is dramatically changed at a first-order O — T′ transition, which exhibits a discontinuous change in the Cu—O_{II}—Cu distance.

B. La_2CuO_4

The fact that the impurity phase encountered in our sample of La_2CuO_4 is ferromagnetic would seem to raise doubts that the localized atomic moment, which is observed consistently in different laboratories, can also be due to an impurity phase, as has been assumed by Saez Puche *et al.* (*15*). This suspicion is reinforced by the close correlation between the low-temperature rise in the electrical resistivity with decreasing temperature and the magnetic anomaly below 200 K. Assignment of the magnetic anomaly to antiferromagnetic order (*15*) is also inconsistent with a Curie law and zero Weiss constant. However, interpretation of the magnetic and transport properties as intrinsic to La_2CuO_4 follows from the band diagram of Fig. 15b.

At temperatures $T > 200$ K, the Curie law is generated by a fixed number of holes in the $d_{z^2}^2$ configuration. Each hole corresponds to a "localized" $d_{z^2}^1$ configuration carrying a spin $S = 1/2$; the electron creating that hole is donated to the $\sigma^*_{x^2-y^2}$ band, which is itinerant with a low density of states at the Fermi energy. At temperatures $T < 200$ K, there is a smooth shifting of the position of the $d_{z^2}^2$ level relative to the Fermi energy, and the number of localized holes decreases monotonically with decreasing temperature. Since the localized holes give rise to a Curie law at $T > 200$ K, they should continue to do so at $T < 200$ K. Therefore Fig. 5a shows the variation in the Curie constant C in emu K/mole; it is constant down to 200 K and then decreases nearly linearly with decreasing temperature below 200 K. The absence of an ESR signal is presumably due to the short lifetime of an $S = 1/2$ state in this mixed-configuration system; and the absence of any interatomic interaction, which would lead to a Weiss constant θ and a Curie–Weiss law, may also be attributed to the mobile character and low concentration of the $S = 1/2$ states.

Assignment of the origin of the shift in the position of E_F relative to the $d_{z^2}^2$ level must be more speculative; a structural refinement below 200 K is needed to test our hypothesis. In view of the distinction between Cu_I^{2+} and Cu_{II}^{2+} ions in La_2CuO_4, it is reasonable to anticipate a shift of the O_{II} ions away from the copper with shorter Cu—O_I bonds toward the copper with a larger Cu—O_I bond. Such a motion would make the average Cu—O distance the same for each type of copper; but it would also change the translational symmetry in the basal plane so as to open up further any energy gap in the middle of the $\sigma^*_{x^2-y^2}$ band. Thus a smooth, cooperative shift of the O_{II} ions that increased in amplitude with decreasing temperature below 200 K would further split the $\sigma^*_{x^2-y^2}$ band and shift the Fermi energy relative to the $d_{z^2}^2$ level as required to make the compound a semiconductor at the lowest temperatures.

The conductivity, $\sigma \simeq 10$ ohm^{-1} cm^{-1}, is temperature-independent, but low for a metallic compound. The lower limit for conductivity in a partially filled band follows from the expression $\sigma = ne^2\tau/m^*$ and the requirement, imposed by the Heisenberg uncertainty principle, that the bandwidth $w = \hbar^2(\pi/a_0)^2/2m^*$ be related to the mean-free time τ between electron scattering events by $\tau > \hbar/w$. For a charge-carrier density $n = c/a_0^3$, it follows that

$$\sigma_{\min} \simeq 0.2g^2c(e^2/\hbar a_0) \simeq c \times 10^2\ \Omega^{-1}\ \text{cm}^{-1} \quad (2)$$

where c is the concentration of mobile charge carriers per copper atom and $g \simeq 1/3$ is the density-of-states reduction factor at the mobility edge (*38*). In this limit the mean-free path between scattering events is about one lattice parameter, which is reasonable in a system with a fluctuating configuration. The mobile electrons tend to become trapped in the localized d_{z^2} orbitals.

On the other hand, it might be preferable, in such a situation, to consider that the

charge carriers move with a diffusive motion, so that $\sigma = ne^2D/kT$. The upper limit for conductivity by this process occurs where the motional enthalpy appearing in the diffusion coefficient is $\Delta H_m < kT$. In this limit, the diffusion coefficient becomes $D \sim a_0^2\nu_0$, where ν_0 is the attempt frequency and a_0 is the jump distance. The maximum room-temperature conductivity in this regime is, therefore,

$$\sigma_{max} \simeq cg^2(h\nu_0/kT)(e^2/\hbar a_0) \simeq 10^3 \times c(h\nu_0/kT) \quad (3)$$

where, for an attempt frequency $\nu_0 \simeq 10^{12}$ sec^{-1}, the room-temperature ratio $(h\nu_0/kT) \simeq 0.1$ makes σ_{min}(band) $\simeq \sigma_{max}$(diffusion).

With either model, it is necessary to assume a small charge-carrier concentration $c \simeq 0.1$ to account for a temperature-independent $\sigma \simeq 10\ \Omega^{-1}\ cm^{-1}$. On the other hand, such a small charge-carrier concentration is consistent with a temperature-independent Seebeck coefficient given by (for small c) $\alpha \simeq -(k/e)\ln c \simeq 200\ \mu V/K$. The positive sign can be attributed to the shape of the combined density of states. Moreover, a concentration $c \simeq 0.1$ of mobile, positive charge carriers agrees with the concentration of localized moments as determined from the Curie constant.

The fact that the number of $\sigma^*_{x^2-y^2}$-band charge carriers is about equal to the concentration of localized spins leads to the conclusion that, even at high temperatures, the $\sigma^*_{x^2-y^2}$ band may be split in two, or nearly so, by the translational symmetry because of the two distinguishable copper atoms in the orthorhombic unit cell. Such a splitting would be increased by cooperative motions of O_{II} atoms in the basal plane below 200 K. This conclusion is also consistent with the apparent lack of any significant temperature-independent term in the magnetic susceptibility. In the absence of any Weiss constant in the temperature dependence of the magnetic susceptibility, there is no basis for postulating an electron-correlation band splitting as was done previously (*7*); but the character of the orthorhombic distortion makes this unnecessary. Moreover, a $\sigma^*_{x^2-y^2}$ band that is too broad to sustain spontaneous magnetization is consistent with the magnetic properties of CuO (30), which indicate itinerant-electron antiferromagnetism, since the Cu—O_{II}—Cu linkages form 180° bonds in La_2CuO_4 and the Cu—O_{II} distance of 1.90 Å is significantly shorter than the 1.95 Å of the short Cu—O bond in Cu—O. The low charge-carrier mobility is well accounted for by configuration fluctuations $d^1_{z^2} \rightleftharpoons d^2_{z^2}$ on the copper ions.

According to the model of Fig. 15b, in which the concentration of mobile $\sigma^*_{x^2-y^2}$-band charge carriers is equal to the concentration of localized spins, the density of charge carriers contributing to the conductivity would decrease approximately linearly with T as does the Curie constant C (see Fig. 5a). As the charge-carrier density decreases, a motional enthalpy $\Delta H_m > kT$ can be expected to affect the mobility, so the resistivity increases more sharply than linearly at the lowest temperatures.

The orthorhombic solid solutions in the systems $La_{2-x}Pr_xCuO_4$, $0 < x < 0.50$, exhibit a thermal variation of the resistivity that is similar to that of the end member La_2CuO_4 (see Fig. 8). The principal evolution with increasing x is a slightly higher conductivity at higher temperatures and a shifting of the onset of the low-temperature rise in resistivity to lower temperatures. This observation shows that the observations on La_2CuO_4 are not sample specific, which is consistent with the localized moments and low-temperature anomalies reflecting an intrinsic material property; it is also consistent with a decrease in all the unit-cell parameters with increasing x, Table I, which would increase the width of the $\sigma^*_{x^2-y^2}$ band.

For all x, a log ρ versus log T plot is linear below 100 K with a slope corresponding to the relation $\rho \sim T^{-2.4}$.

C. La_2NiO_4

The magnetic susceptibility of La_2NiO_4 shows a Curie–Weiss law at high temperatures that is compatible with the energy diagram of Fig. 14 and strong correlations among the $\sigma^*_{x^2-y^2}$ electrons. A Weiss constant $\theta < 0$ indicates antiferromagnetic coupling in accordance with the superexchange rules for interactions between half-filled $d_{x^2-y^2}$ orbitals—or for correlations in a half-filled $\sigma^*_{x^2-y^2}$ band (*28*). From Table II, the high-temperature $\mu_{eff} = 3.03\ \mu_B$ is a little larger than the spin-only value $2.83\ \mu_B$ that would be expected for a localized-electron S = 1 configuration and a constant Weiss molecular-field parameter W. On the other hand, the low-temperature ($T < T_d$) susceptibility gives a measured $\mu_{eff} = 1.83\ \mu_B$, which is closer to the localized-electron $S = 1/2$ value of $1.73\ \mu_B$. Since the low-temperature susceptibility is field-independent, there is no evidence of a weak ferromagnetism below T_d, which agrees with the neutron-diffraction data. We seem forced to conclude that below T_d the strong correlations among the $\sigma^*_{x^2-y^2}$ electrons have either collapsed or changed their character so as not to provide interatomic interactions.

If the correlations among the itinerant $\sigma^*_{x^2-y^2}$ electrons are induced only by intraatomic-exchange coupling to the "localized" d_{z^2} electrons, then the magnetic susceptibility may only asymptotically approach a localized-electron Curie–Weiss law at the highest temperatures as shown in Fig. 16 (*28*). In this case, a measured μ_{eff} larger than the theoretical μ_{eff} would be obtained from lower temperature susceptibility data, and the magnitude of the Weiss constant θ would be high relative to any observed magnetic-ordering temperature T_N. Since μ_{eff} is larger than the theoretical value for $T > T_d$, we may assume that the measured Weiss constant $\theta = -500$ K may be somewhat larger in magnitude than could be expected from the strength of the

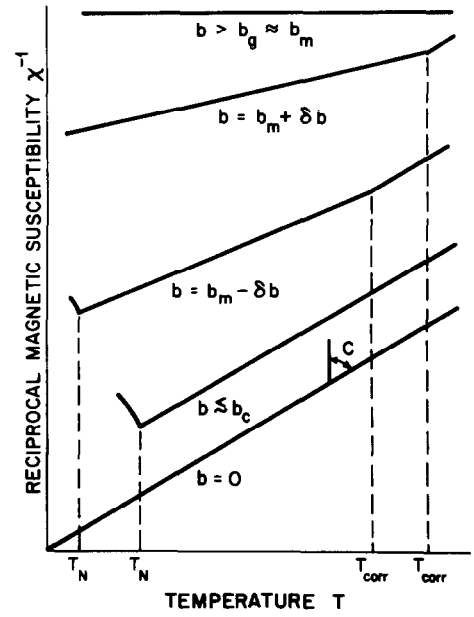

FIG. 16. Predicted variations with b in the temperature variation of the inverse paramagnetic susceptibility for $n_l = 1$, after Ref. (*28*).

interatomic exchange interactions.

The smooth, but abrupt collapse in the contribution of the $\sigma^*_{x^2-y^2}$ electrons to the magnetic susceptibility implies that a spin pairing among the $\sigma^*_{x^2-y^2}$ electrons is stabilized relative to an enhancement of the electron correlations via intraatomic exchange interactions. Moreover, the spin pairing cannot be a long-range antiferromagnetic order as the localized d_{z^2} moments remain decoupled. Such a situation could occur were there a disproportionation among the narrow-band $\sigma^*_{x^2-y^2}$ electrons that was brought about by a cooperative displacement of the in-plane O_{II} atoms toward one set of nickel atoms and away from another. Unless such displacements are accompanied by a distortion to orthorhombic symmetry at low temperatures of the type found in La_2CuO_4, the disproportionation would represent a two-dimensional charge-density wave in which the disproportionation reaction

$$2Ni^{2+} \rightarrow Ni_I^{(2+\delta)+} + Ni_{II}^{(2-\delta)+} \quad (4)$$

occurs. Lack of long-range ordering between basal planes could have obscured observation of a doubling of the basal plane of the unit cell in the neutron-diffraction experiments (*20*).

Nevertheless, such a speculation does not account for the apparent absence of any evidence of antiferromagnetic ordering—even short-range—down to 12 K in the presence of a low-temperature $\theta \simeq -120$ K.

At $T_{min} \simeq 600$ K, the resistivity has a minimum value; it corresponds to a $\sigma_{min} \simeq 35$ Ω^{-1} cm^{-1} for the metallic phase at temperatures $T > T_{min}$, which is in good accord with Eq. (2). At lower temperatures, an activation energy $E_a = 0.053$ eV $\simeq kT_{min}$ suggests a motional enthalpy is responsible for the observed activation energy: $E_a = \Delta H_m$. Such a situation is quite compatible with strong correlations among the $\sigma^*_{x^2-y^2}$ electrons that are induced by intraatomic-exchange interactions with localized d_{z^2} electrons. The charge-carrier mobility would be reduced by the formation of small magnetic polarons. However, the increase in activation energy below T_d, although small (E_a = 0.082 eV), must be correlated with an apparent collapse in the contribution of the $\sigma^*_{x^2-y^2}$ electrons to the paramagnetic susceptibility. Whatever is pairing the $\sigma^*_{x^2-y^2}$ electrons below T_d appears to be opening up an energy gap that splits occupied from empty band states. Stabilization of the charge-density wave discussed above would accomplish this.

The above discussion is based on the assumption that the apparent Curie–Weiss law below T_d is meaningful and that a $\mu_{eff} \simeq 1.83\ \mu_B$ taken from the slope of the χ_m^{-1} versus T curve in this temperature range is not fortuitous, but is a measure of the atomic moment at magnetically disordered nickel atoms. To test this assumption, it is useful to investigate some solid solutions with La_2NiO_4.

D. $La_2Ni_{1-x}Cu_xO_4$

Substitution of copper for nickel in the tetragonal-T phase gives a paramagnetic susceptibility per Ni^{2+} ion similar to that found in La_2NiO_4. However, the measured μ_{eff} at high temperatures decreases toward the theoretical value with increasing x as though the $\sigma^*_{x^2-y^2}$ band were being narrowed by the introduction of foreign cations. The initial increase in c/a ratio with x signals that the Cu^{2+} ions have a $d^2_{z^2}$ configuration stabilized below the Fermi energy, which would account for the lack of any contribution to the magnetic susceptibility from the copper. With a diamagnetic $d^2_{z^2}$ configuration, there is no local moment to magnetize the $\sigma^*_{x^2-y^2}$ electrons at a Cu^{2+} ion. This introduces a reduction in the stabilization of the high-temperature state having correlated $\sigma^*_{x^2-y^2}$ electrons, so T_d increases with x. At the same time T_d becomes less well defined. However, the $x = 0.25$ sample still shows a break in the resistivity at T_d (see Fig. 5a). Below T_d, the μ_{eff} remains close to the theoretical value of $S = 1/2$ per Ni^{2+} ion, which would seem to confirm the hypothesis that only the $d^1_{z^2}$ configurations are contributing to the magnetic susceptibility. Further support comes from the observation (Table II and Fig. 6) that the $x = 0.75$ sample shows a larger μ_{eff} at low temperatures. Given the band diagram of Fig. 15b for La_2CuO_4, this enhancement would seem to indicate the introduction of holes into the $d^2_{z^2}$ level at the Cu^{2+} ions at higher copper concentrations and hence the prefiguration of a distortion from the T to the O structure. Indeed, the O structure is found at room temperature in the $x = 0.9$ sample.

Thus the behavior of the system $La_2Ni_{1-x}Cu_xO_4$ makes good contact with the models proposed for the two end members. Moreover, it would appear that the transition at T_d in the T phase and that at 200 K in La_2CuO_4 have a common crystallographic origin. For each we have postulated the for-

mation of a charge-density wave in the $\sigma^*_{x^2-y^2}$ bands as the result of a cooperative displacement of the O_{II} atoms.

E. $La_{2-2x}Sr_{2x}Ni_{1-x}Ti_xO_4$

The tetragonal-T system $La_{2-2x}Sr_{2x}Ni_{1-x}Ti_xO_4$ has a magnetic susceptibility per Ni^{2+} ion that is very similar, for $0 < x < 0.5$, to that of the system $La_2Ni_{1-x}Cu_xO_4$ with the same values of x, see Fig. 6a. As can be seen from Table II, the high-temperature μ_{eff} approaches the theoretical value of 2.83 μ_B for $S = 1$, and the high-temperature Weiss constant θ decreases with increasing x. Although T_d is not sharply defined in either system, the low-temperature susceptibility has a continuous change of slope of the χ_m^{-1} versus T curve that seems to approach asymptotically a Curie law. Moreover, the high-temperature activation energy in the resistivity increases with x as might be expected for narrower $\sigma^*_{x^2-y^2}$ bands.

The $x = 0.75$ sample, which is beyond the percolation limit $x = 0.59$ for a square-planar net (*31*), has a quite different character: it exhibits a simple Curie law with $\mu_{eff} = 2.73\ \mu_B$ for all temperatures, and the sample is a better semiconductor (see Fig. 9) with the typical green color of a Ni(II) oxide. Thus the existence of a T_d and of a high-temperature Weiss constant θ is clearly associated with Ni—O_{II}—Ni interactions. The fact that the Ni^{2+} and Ti^{4+} ions remain disordered in the $x = 0.5$ sample is itself unusual; it may reflect a stabilization associated with Ni—O_{II}—Ni interactions and/or the disorder of the La^{3+} and Sr^{2+} ions.

If T_d in La_2NiO_4 reflects a cooperative displacement of O_{II} atoms within a basal plane, then it would appear, from the blurring of T_d, that the atomic displacements are only short-range cooperative in the mixed systems.

F. The T′ Phase

In the T′-tetragonal phases Pr_2CuO_4 and Nd_2CuO_4, the significantly larger Cu—O_{II}—Cu distance will narrow the $\sigma^*_{x^2-y^2}$ band, and the removal of the O_I atoms to tetrahedral interstices of the Ln_2 bilayer guarantees a $d^2_{z^2}$ state completely below the Fermi energy E_F as pictured in Fig. 15a. The observation of an activation energy in the resistivity of 0.069 eV with $T_{min} \simeq 700$ K, see Fig. 9a, indicates that the $\sigma^*_{x^2-y^2}$ electrons are probably strongly correlated, but it is nevertheless dangerous to assume that, because the copper makes no apparent contribution to the susceptibility below 300 K, it must be antiferromagnetically coupled (*16*). It would be useful to have neutron-diffraction data to clarify this point.

G. Random Comments

In a previous communication, one of us (*21*) suggested that the resistivity minimum occurring in high-temperature La_2NiO_4 might be due to a suppression of the electron correlations in the $\sigma^*_{x^2-y^2}$ band as a result of an increase in the c/a ratio with temperature. However, it is more probably due to an $E_a \simeq \Delta H_m$ becoming $\Delta H_m < kT$, as discussed in connection with Eq. (3). In the present study, we have found no correlation between the resistivity minimum and changes in the c/a ratio. Moreover, the electronic conductivity appears to be better described by a diffusive motion.

The ESR signals observed from the system $La_{2-x}Pr_xCuO_4$ are not necessarily associated with Cu^{2+} ions in the host structure. Oxygen vacancies containing a single electron must also be considered. It does not appear relevant to the present study to attempt to sort out the assignments of the various signals observed.

The observation of a magnetic susceptibility that obeys a Curie–Weiss law to lowest temperatures with no apparent magnetic ordering, as we report for La_2NiO_4, is not completely without precedence in oxides, but it has not previously been noted. It can be seen, for example, in the magnetic-sus-

ceptibility data reported for the bronze $Na_{0.33}V_2O_5$ (*32*) and for $LaSrCoO_4$ (*33*), both low-dimensional systems. Such a behavior has also been observed in the valence-fluctuation systems $LnCu_2Si_2$ (*34*); in this case, a quasi-Boltzmann partition function has been invoked to account for it (*35*).

Acknowledgment

J. B. Goodenough thanks the Indian Academy of Sciences for a Raman Visiting Professorship.

References

1. M. Foex, *Bull. Soc. Chim. Fr.* 109 (1961).
2. V. A. Rabenau and P. Echerlin, *Acta Crystallogr.* **11,** 304 (1958).
3. R. J. Birgenau, J. Shalo, and G. Shirane, *J. Appl. Phys.* **41,** 1303 (1970).
4. J. M. Longo and P. M. Raccah, *J. Solid State Chem.* **6,** 526 (1973).
5. P. Ganguly and C. N. R. Rao, *Mater. Res. Bull.* **8,** 408 (1973).
6. T. Kenjo and S. Yajima, *Bull. Chem. Soc. Jpn.* **46,** 1329 (1973).
7. J. B. Goodenough, *Mater. Res. Bull.* **8,** 423 (1973).
8. H. Müller-Buschbaum and W. Wollschlager, *Z. Anorg. Allg. Chem.* **414,** 76 (1975).
9. T. Kenjo and S. Yajima, *Bull. Chem. Soc. Jpn.* **50,** 2874 (1977).
10. U. Lehmann and H. Müller-Buschbaum, *Z. Anorg. Allg. Chem.* **470,** 59 (1980).
11. C. Chaumont, G. Le Flem, and P. Hagenmuller, *Z. Anorg. Allg. Chem.* **470,** 18 (1980).
12. R. Berjoan, J. P. Contures, G. Le Flem, and M. Saux, *J. Solid State Chem.* **42,** 75 (1982).
13. V. B. Grande, H. Müller-Buschbaum, and M. Schweizer, *Z. Anorg. Allg. Chem.* **428,** 120 (1977).
14. P. Ganguly, S. Kollali, and C. N. R. Rao, "Proceedings, Nuclear Physics and Solid State Phys. Symposium, Bombay, India," No. 21c, 603 (1978).
15. R. Saez Puche, M. Norton, and W. S. Glaunsinger, *Mater. Res. Bull.* **17,** 1429 (1982).
16. R. Saez Puche, M. Norton, and W. S. Glaunsinger, *Mater. Res. Bull.* **17,** 1429 (1982).
17. V. B. Grande and H. Müller-Buschbaum, *Z. Anorg. Allg. Chem.* **433,** 152 (1977).
18. R. D. Shannon and C. T. Prewitt, *Acta Crystallogr. B* **25,** 925 (1969).
19. G. A. Smolenskii, V. N. Yudin, and E. Sher, *Sov. Phys. Solid State* **4,** 2452 (1963).
20. G. A. Smolenskii, V. A. Bokov, S. A. Kizaev, E. I. Maltzev, G. M. Nedliev, V. P. Plankty, A. G. Tutov, and V. N. Yudin, "Proceedings, International Conference on Magnetism, Nottingham, 1964," p. 354, Inst. Phys. and Phys. Soc., London (1965).
21. J. B. Goodenough and S. Ramasesha, *Mater. Res. Bull.* **17,** 383 (1982).
22. K. K. Singh, P. Ganguly, and C. N. R. Rao, *Mater. Res. Bull.* **17,** 493 (1982).
23. P. Ganguly, S. Kollali, C. N. R. Rao, and S. Kern, *Magn. Lett.* **1,** 107 (1980).
24. A. Mehran and D. J. Machin, *J. Chem. Soc. Dalton Trans.* **1975,** 1061.
25. S. Kollali, D. Phil. thesis, Bangalore, India (1980).
26. B. J. Hathaway and D. E. Billing, *Coord. Chem. Rev.* **5,** 141 (1970).
27. P. Poix, *J. Solid State Chem.* **31,** 95 (1980).
28. J. B. Goodenough, *in* "New Developments in Semiconductors" (P. R. Wallace, R. Harris, and M. J. Zuckermann, Eds.), p. 105, Noordhoff, Leyden (1973).
29. M. P. Dare-Edwards, J. B. Goodenough, A. Hamnett, and N. D. Nicholson, *J. Chem. Soc. Faraday Trans. 2* **77,** 643 (1981).
30. M. O'Keeffe and F. S. Stone, *J. Phys. Chem. Solids* **23,** 261 (1962).
31. B. K. Shante and S. Kirkpatrick, *Advan. Phys.* **20,** 325 (1971).
32. M. K. Sienko and J. B. Sohn, *J. Chem. Phys.* **44,** 1369 (1966).
33. G. Demazeau, P. Courbin, G. Le Flem, M. Pouchard, P. Hagenmuller, J. L. Sonteyroux, I. G. Main, and G. A. Robin, *Nouv. J. Chim.* **3,** 171 (1979).
34. B. C. Sales and R. Viswanathan, *J. Low-Temp. Phys.* **23,** 449 (1976).
35. B. C. Sales and D. K. Wohlleban, *Phys. Rev. Lett.* **35,** 1240 (1975).
36. B. Willer and M. Daire, *C.R. Acad. Sci. C* **267,** 1482 (1968).
37. D. Reimen and C. Friebel, *Struct. Bonding* **37,** 1 (1979).
38. N. F. Mott, *Philos. Mag. B* **44,** 265 (1981).
39. J. B. Goodenough, "Magnetism and the Chemical Bond," p. 122, Wiley–Interscience, New York (1963).